Exploiting Simultaneous Multi-Band Operation to Improve 6TiSCH Reliability and Latency

Marcus Vinicius Bunn, Samuel Baraldi Mafra, Richard Demo Souza, Guilherme Luiz Moritz

***Abstract*—The Internet Engineering Task Force (IETF) group "IPv6 over the TSCH mode of IEEE 802.15.4e" (6TiSCH) introduced a protocol, utilizing Time-Slotted Channel Hopping (TSCH) from IEEE802.15.4e due to its high reliability and time-deterministic characteristic, that achieves industrial performance requirements while offering the benefits of IP connectivity. This work proposes the addition of a second radio interface in 6TiSCH devices to operate a parallel network in sub-GHz, introducing transmit diversity while benefiting from decreased path-loss and reduced interference. Simulation results show an improvement of 20% in Packet Delivery Ratio (PDR) and close to 31% in latency in different 6TiSCH networks scenarios.**

***Index Terms*—Industrial IoT, Multi-band, sub-GHz, 6TiSCH.**

I. Introduction

The Industry 4.0 paradigm promises unprecedented improvements in productivity, control, maintenance and cost reduction to factories and industries, while enabling the development of new products and processes [2]. One of the main technologies supporting this evolution is the Industrial Internet of Things (IIoT) [3], enhancing factory connectivity levels, powering varied applications and integrating Wireless Sensor Networks (WSN) with the Internet. A major challenge is to guarantee the communication requirements in terms of determinism, latency and reliability for critical industrial applications [4]. For many years the increased reliability of wired networks has suppressed the benefits of mobility, flexibility and cost reduction of wireless networks [5], leaving wireless deployments for secondary systems [6].

A set of industrial communication protocols have been designed to address the above challenges, such as WirelessHART [7], ISA100.11a [8] and WIA-PA [9]. These protocols are based on the Time-Slotted Channel Hopping (TSCH) mode of IEEE802.15.4e [10], due to its high reliability and time-determinism. By delivering 99.999% end-to-end reliability and over a decade of battery lifetime [11], TSCH has become the *de-facto* Medium Access Control (MAC) technique for industrial applications [12]. Moreover, the continuous increase in prediction of future connected devices, and the proven applicability of the IIoT to fulfill the Industry 4.0 requirements [13], encouraged the creation of the Internet Engineering Task Force (IETF) group "IPv6 over the TSCH mode of IEEE 802.15.4e" (6TiSCH). Their efforts resulted in a communication protocol capable of achieving industrial performance requirements while offering the benefits of IPv6 connectivity [14].

However, wireless communication in rough industrial environments remains challenging, due to interference and fading. Interference may be caused by other technologies, by a secondary deployment, or between devices in the same network, while fading is inherent to the wireless link [15]. TSCH increases network performance over multi-path fading and interference, but the continuous increase in connected devices combined with the strict reliability and latency requirements of the Industry 4.0 paradigm [16] pose new challenges. Therefore, existing and continuous efforts from the industry and academia are required to improve IIoT networks performance.

Some related work aim at improving TSCH via redundant transmissions [17], [18] and the usage of sub-GHz band with multi-band support [19], [20]. However, it is noticeable the absence of a single approach that combines both methods, and which can improve TSCH network performance against interference and multi-path fading. In this context, this work proposes the addition of a second radio interface in 6TiSCH devices to operate a parallel network in sub-GHz band, as depicted in Fig. 1. The method brings significant advantages by improving reliability, capacity, channel utilization, coverage, load balancing, and interoperability, while it can be used in several contexts like Disruption Tolerant Networks [21], Wireless Mesh Networks [22] and recent IoT protocols like TSCH [14]. The results of several simulations show potential improvements of up to 25% in Packet Delivery Ratio (PDR) and closely to 30% in latency in different tests, at the cost of increased hardware complexity.

It is important to highlight that this work is an extended version of [1], including updated discussion related to the state of the art, as well as results from additional tests to provide insights on the effect of different node distances and the contribution of each band in the overall performance.

The rest of this work is organized as follows. Section II discusses related work, while Section III introduces the system model. Section IV describes the proposed method and the performance metrics. The simulation methodology is presented in Section V, while simulation results are discussed in Section VI. Finally, Section VII concludes the paper.

M.V. Bunn and R.D. Souza are with the PPGEEL, Federal University of Santa Catarina (UFSC), Florianopolis-SC, Brazil (e-mail: bunnmv@gmail.com, richard.demo@ufsc.br)

G.L. Moritz is with the PPGSE, Federal University of Technology-Parana, Curitiba-PR, Brazil (e-mail: moritz@utfpr.edu.br)

S.B. Mafra is with the National Institute of Communications of Brazil (INATEL), Santa Rita do Sapucai-MG, e-mail: samuelbmafra@inatel.br

This work is an extended version of [1], which was presented in the XL Brazilian Telecommunications and Signal Processing Symposium (SBrT2022). This work has been partially supported by CNPq and CAPES.

This work was partially funded by Brazilian National Council for Scientific and Technological Development - CNPq, grant 402378/2021-0.

Digital Object Identifier: 10.14209/jcis.2023.18

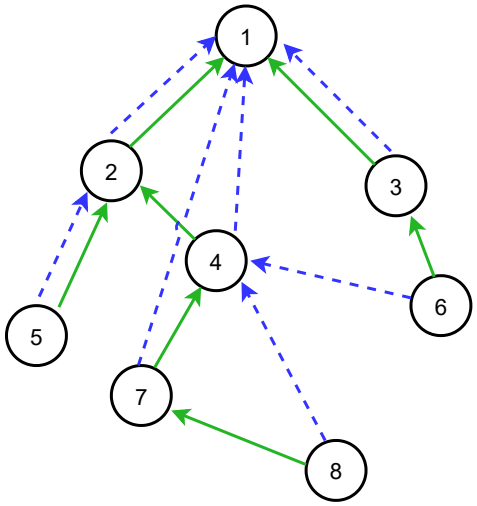

Fig. 1: Multiband operation proposed in this work. Two single band network topologies, one operating in the 868MHz band (blue dashed lines) and other operating in the 2.4GHz band (green solid lines) can be combined to form a multiband topology where each transmitter packet experience diversity effects by being transmitted simultaneously in both bands using two different paths. Results show that multiband operation can significantly improve packet delivery ratio and latency when compared with the single band networks.

II. Related Work

A. 6TiSCH Overview

The IETF IPv6 over the TSCH mode of IEEE802.15.4e (6TiSCH) Working Group (WG) has been established to produce specifications of an interoperable stack integrating IEEE802.15.4e TSCH to IETF solutions targeting IoT applications [14]. The stack uses the IEEE802.15.4 physical layer (PHY) operating in the 2.4 GHz (ISM) band. This band is divided in 16 channels [10] whose use is governed by the Time Slotted Channel Hopping (TSCH) IEEE802.15.4e mode, which combines Time Division Multiple Access (TDMA) with channel hopping to create a collision free environment which can increase reliability over multi path fading and interference. Additionally, 6TiSCH provides a set of management protocols that enables plug-and-play bootstrap, authentication and wireless medium management [23]–[27].

In the 6TiSCH stack, communication occurs in specific times while obeying a maximum duration determined by a *timeslot*. Timeslots repeat in time indefinitely and a group of timeslots is named a *slotframe*. A scheduling function determines whether a node is transmitting, receiving or sleeping in each timeslot, which can offer deterministic and reliable communication with improved battery lifetime by allowing nodes that are not transmitting or receiving to enter in sleep mode. The resulting allocation, named schedule, can be viewed as a repeating $M \times N$ matrix, where M is the number of available physical channels and N is the slotframe length, as depicted in Fig. 2. Channel hopping is achieved by selecting offsetting channel cells in each slotframe iteration [28].

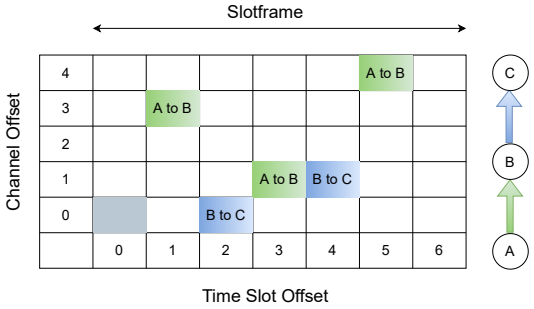

Fig. 2: A 6TiSCH schedule example. The slotframe contain 7 timeslots and 5 physical channels. Cells are mapped to a execution time and channel frequency based on time (0 to 6) and channel (0 to 4) offset. The gray timeslot is reserved for broadcast while green and blue timeslots represent unicast communication from Node A to B and from Node B to C, respectively.

To provide a zero configurarion network, the 6TiSCH minimal configuration [26] defines a mandatory basic schedule which must be followed by any 6TiSCH node. This minimal schedule provides basic message exchange that can be used in conjunction with the 6TiSCH Operation Sublayer (6top) Protocol (6P) [27] to negotiate more complex communication schedules governed by a Scheduling Function (SF). A mandatory basic Schedule function, named Minimal Scheduling Function (MSF) [24] is provided by 6TiSCH.

After single link communication is established, routing is provided by RPL [29], which defines four types of messages to create a directed acyclic graph (DAG) towards the root. A new node that wants to join the network (named pledge) must listen to messages carrying DODAG joining information (DIO) which are periodically broadcast by the network and can also be actively solicited by the pledge using DODAG information solicitation messages (DIS). Upon receiving DIO messages from multiple nodes, a pledge uses an Objective Function to choose a parent that will be the first hop of all the pledge messages. This function is implemented to achieve specific requirements, as to increase network lifetime and avoid loops [30]. To complete the joining procedure, the selected parent must be addressed with a destination advertisement object (DAO) message which is replied by a DAO acknowledge (DAO-ACK) in the case of a joining accept.

At the transport and network layers, 6TiSCH stack uses IPv6 over Low-Power Wireless Personal Area Networks (6LoWPANs) [31] to compress User Datagram Protocol (UDP) and IPv6 headers. In the application layer it uses Constrained Application Protocol (CoAP) [32], secured by a tool called Object Security for Constrained RESTful Environments (OSCORE) [33]. The 6TiSCH minimal configuration defines the Constrained Join Protocol (CoJP) for a secure joining process. The process is executed in a single transaction, where the pledge sends authentication data to one available neighbor, named Join Proxy (JP) that is forwarded to the Join Registrar/Coordinator (JRC). Transactions are executed after RPL join process is initiated and encrypted keys are sent over the

minimal cell for authentication. If approved, the JRC notifies the pledge to confirm its addition to the network.

B. Redundant Transmission, Sub-GHz Operation and Multi-Band Support

This subsection discusses related work that use the TSCH mode of IEEE 802.15.4e and that propose redundant transmission, sub-GHz operation and multi-band support.

Minet et al. [17] exploit redundant transmissions that benefit from different communication links to increase reliability, where a node sends a message through multiple paths depending on a redundancy pattern. The sink node accepts the first delivered message and discards the late copies, which increases reliability and reduces latency. The increase in reliability is achieved at the cost of additional network overhead that decreases battery lifetime. Moreover, additional studies would be required to confirm the effectiveness of the proposed strategy on interference prone environments with coexisting networks, where redundant transmissions could degrade performance by increasing network density and interference levels.

Papadopoulos et al. [18] propose redundant transmissions associated with an overhearing mechanism to increase reliability and reduce latency. Each node forwards its messages not only to the default RPL parent but also to a redundant parent. In addition, packet retransmissions due to incorrect receptions are eliminated. Simulation results were compared against the default TSCH-RPL network using different retransmission levels, demonstrating a reduction of up to 54% in end-to-end latency and 84% in jitter when compared with a non redundant scenario with 8 retransmissions at the cost of increased energy consumption caused by the redundant transmissions. Regarding PDR, results showed no improvements when compared to the the retransmission approaches, and the authors justify this behavior by stating that the removal of retransmissions negatively impacted the control packets reliability.

Yin, et al. [19] tackles the interference problem on WSNs that operate in the 2.4 GHz band caused by popular WiFi and Bluetooth network deployments by proposing dual band operation. The scheme performs sequential transmissions for both 900 MHz and 2.4 GHz. Experiments were conducted to evaluate the proposed scheme performance on two different testbeds [34], [35]. The PDR is selected as evaluation metric and tests are executed over varied wireless channels from 900 Mhz to 2.4 GHz. Results show that the average PDR was approximately 5% higher in the 900Mhz band, while also improving the connectivity by 15%, when compared to the 2.4 GHz band. It concludes, based on experimental results, that the presented scheme can be used to increase network performance and connectivity, although the paper focuses only on the physical/link layers.

Brachmann, et al. [20] propose multiple frequency and bitrates in a single IEEE 802.15.4e TSCH schedule to meet multiple application requirements by trading datarate with robustness. Two approaches are investigated, the first assigning timeslots duration to accommodate the slowest transmission and the second allowing slower transmissions to use several timeslots. The performance of the proposed schemes were evaluated experimentally using 25 nodes deployed in an office environment. For the tests, TSCH control data was transmitted in the sub-GHz band that offer increased reliability while application data is transmitted over 2.4 GHz to achieve faster delivery times. The usage of sub-GHz bands granted single-hop reaches close to 24 nodes at 1.2kbps, while at the standard 250kbps in 2.4 GHz the reach decreases drastically to an average of 10 nodes. Results also showed that the 1.2 kbps band at sub-Ghz has a 20x higher channel utilization when compared to the 2.4GHz band at 1000 kbps, while improving network synchronization by reducing the required average hops for control data. The work successfully demonstrates the required timing configuration required in TSCH networks to operate in sub-GHz and allows multi-band operation.

Van Leemput et al. [36] proposed a multi-phy TSCH network where the rate of the unicast links is lowered when the average of the Received Signal Strength Indicator (RSSI) drops below a preconfigured threshold. To accommodate the slower PHYs, the author breaks compatibility with the 802.15.4e standard by allowing a node to transmit more than one packet on a timeslot. This way, the network can be configured to use a long enough timeslot to allow a slower PHYs transmission and acknowledgment reception without the bandwidth penalty that would be imposed to the faster PHYs if only one transmission per slot were used. Using this scheme, the authors claim a throughput increase of 153%.

A similar link-by-link PHY switching basis is evaluated in [37], where it is stated that their technique allows the radio to use a more energy efficient interface when possible, switching to a more reliable but more power hungry when needed. Results show that the strategy yields lower latency and network formation time than any of the individual used PHYs. This work was extended in [38] where a RPL objective function was developed to use the strategy previously proposed in [37]. Results demonstrate that the approach may lead to a better balanced network, where nodes uses short range 2.4GHz interfaces when power consumption must be reduced in contrast to the standard RPL objective function which tends to converge to a pure long-range network, leading to short network lifetime. On the other hand, the proposed solution has an important disadvantage since is not compatible with the IETF 6TiSCH specification.

Against the above background, we propose the simultaneous use of multi-band interfaces. Our solution utilizes 2.4 GHz and sub-GHz networks like [18]–[20], but we apply redundant transmissions and exploit diversity in a more "standard" fashion, where redundancy occurs naturally by using the additional operating band combined with frequency and spatial diversity associated with the different TSCH and RPL networks. Our method is simpler to implement than [37], since no modifications to the communication stack are required. As an additional advantage, the proposed method allow multiband nodes to communicate with single band devices from any of the supported PHYs, which allows the deployment of a hybrid network where the less energy efficient and more complex multiband nodes are used only when needed, seamlessly communicating with single band devices.

III. System Model

We assume that N static nodes are distributed in a 2D square surface of side L. The nodes may be randomly or uniformly distributed in the area. The nodes collect data periodically and transmit them to the DODAG root, abiding by the TSCH scheduling for that frequency band and by the RPL configuration. In the so called Linear topology, nodes are at equal distance from their neighbors in both directions, except for the DODAG root, which is positioned at the center in coordinates ($L/2$, $L/2$). In the so called Random topology, nodes are positioned randomly and the only requirements are: 1) the DODAG root is at the center; 2) all nodes must be within the area; and 3) nodes must have at least one reachable neighbor. The MSF determines when communication occurs for each node to its neighbor at every hop in the RPL DAG. If no cells are available for one node to communicate with its neighbor, the transmission is scheduled for the next slotframe, where MSF will control if additional communication timeslots are required. Communications may occur in two different frequency bands: 868 MHz and 2.4 GHz.

The effects of distance between nodes and propagation loss are taken into account according to the Pister-Hack [39] model, where the path loss is uniformly distributed between that obtained from the Friis equation (free space) and Friis plus 40 dB. The resulting values are used as a link quality metric, such as DAG formation and for calculating packet reception probability [40]. To determine reception probability, RSSI values are first converted to PDR values based on a conversion table. Moreover, the interference modeling considers the signal-to-interference-plus-noise ratio (SINR), which is calculated by adding the RSSI from the interfering neighbors to the background noise.

IV. Proposed Method and Performance Metrics

This work proposes multi-band support in 6TiSCH by employing two independent radio interfaces with concurrent transmissions. At first glance this option may look prohibitive because it can raise hardware complexity, but the increment can be mitigated by the use of a dual band radio like AT86RF215 [41]. In this configuration, a single chipset may transmit in both proposed bands and only a second RF frontend need to be added. Since the costs of this frontend is relatively small, the solution can be very effective in providing extra coverage with low impact on the hardware costs.

The 2.4GHz band uses the IEEE 802.15.4e PHY specification with 16 channels, each spaced by 5MHz, and transmits at 250kbps rate. At this rate, within a 10ms TSCH timeslot it is possible to transmit a data frame and to receive an acknowledgment [20]. The sub-GHz band follows the IEEE 802.15.4g-2012 standard [42] configuration using the Operating Mode #1 for the 863-870MHz band in Europe which is specified for 50kbps transmission rate and 200kHz channel spacing in a total of 34 available channels. Due to the slower transmission rate, the timeslot timing must be adapted. Then, since there is no standard value in the IEEE specification, we elected 29.38ms as in [20, Table III], mainly because of their proven efficiency and thorough tests.

The two interfaces can be exploited in at least two approaches. The first is by means of a common topology where a node chooses the transmitting band in a per hop fashion. The second is by forming an independent routing topology for each band, and then, when a packet is generated, scheduling it for transmission in both interfaces as soon as possible. The actual transmit time may be different for each interface due to the independence between timeslot duration and scheduling configurations in different bands. Using a common topology is more energy efficient, but imposes some disadvantages. The first one is the fact that dual band operation is not supported by the 6TiSCH specification, which breaks compatibility of each node running the dual band stack. In addition, routing algorithms in dual band mode are more complex, which may be undesirable in resource constrained nodes. Finally, since the packet is only sent using one interface, there is no diversity benefit from multiple paths. For this reason, this work uses the dual topology strategy, where each message traverses two routing paths.

By using diverse paths to the DAG root, we envision that it is possible to improve the overall performance in terms of PDR and latency simultaneously due to the introduction of frequency diversity, reduced interference and increased robustness. Due to this design choice, a packet may take different paths towards the root in each band and no packet replication and elimination can be implemented at intermediate nodes, as this would eliminate the end-to-end path diversity gains. On the other hand, our proposed network uses replication provided by the usual retransmission methods implemented in TSCH, and deduplication at the destination is an already implemented technique in networks relying on UDP connections, where duplication is likely by design.

A. Performance Metrics

In the following sections, some performance metrics that are used to ensure reliable, deterministic and time-sensitive communication for industrial applications are defined.

1) PDR: Consider $\mathcal{S}$ a set containing $|\mathcal{S}| = N$ nodes in a simulation run. Next, consider $\mathcal{M}^{\text{Tx}}$ the set of generated messages by all nodes $\in \mathcal{S}$. Each packet $p \in \mathcal{M}^{\text{Tx}}$ is transmitted to the root node using all the available interfaces of the generating node. To be considered correctly received, p must arrive correctly in at least one of the DAG root wireless interfaces. A packet may be lost due to effects of the wireless medium, consequently, only a subset of $\mathcal{M}^{\text{Tx}}$, denoted $\mathcal{M}^{\text{Rx}}$ is correctly received. The network PDR can be defined as:

$$\text{PDR} = \frac{|\mathcal{M}^{\text{Rx}}|}{|\mathcal{M}^{\text{Tx}}|}. \tag{1}$$

Transmitting using multiple interfaces at different frequencies increases the PDR since each packet follows a different path, having a lower probability of being in outage simultaneously than each one individually, as illustrated in Fig. 3. Note that node A is relatively distant from its parent node C, what inflicts greater path-loss and therefore a higher packet loss probability when compared to Node B (which is closer to the parent node C). The network benefits from the transmission diversity introduced by the sub-GHz interface, as in the example provided

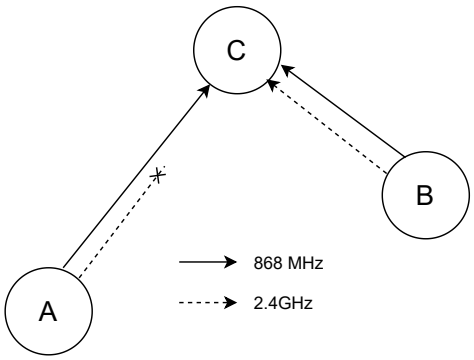

Fig. 3: Node A distance to its parent C inflicts greater path-loss and higher packet loss probability when compared to Node B. Packets are transmitted simultaneously in both radio interfaces where only the packet from the sub-GHz band is effectively decoded at C. The network benefits from the transmission diversity introduced by the sub-GHz interface.

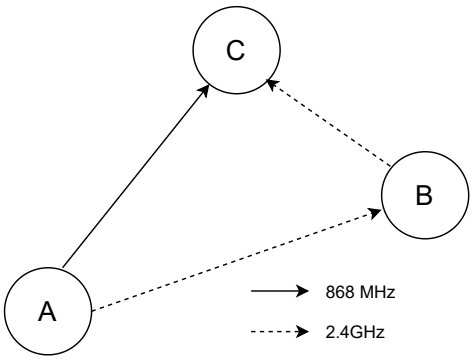

Fig. 4: Node A simultaneously sends a packet by both interfaces, with different RPL topologies and TSCH scheduling. In the 2.4Ghz interface, Node A transmits the packet to its parent B, which then relays to the destination C. In the 868Mhz interface, the packet is directly transmitted from A to C. Sub-GHz bands allow longer hops, reducing latency by eliminating multiple scheduling and transmission processes in packet forwarding.

in Fig. 3 the packet sent through the 2.4 GHz interface from node A to C was lost, while its replica transmitted using the more reliable sub-GHz interface was successfully received.

2) Latency: Consider t_p^{Tx} the time when a packet $p \in \mathcal{M}^{\text{Rx}}$ is generated at node $i \in \mathcal{S}$, while t_p^{Rx} is the time when this same packet p firstly arrives at any of the DAG root interfaces. The average network latency L is

$$L = \frac{\sum_{p \in \mathcal{M}^{\text{Rx}}} \left[t_p^{\text{Rx}} - t_p^{\text{Tx}} \right]}{|\mathcal{M}^{\text{Rx}}|}. \quad (2)$$

Fig. 4 illustrates the benefit in latency that can be introduced by the usage of sub-GHz bands when the amount of average hops is decreased. Additionally, revisiting Fig. 3 it can be noticed how latency can also be improved by reducing packet retries, where a successful communication is executed by the sub-GHz band while the 2.4GHz would require multiple retries to complete the transmission. In both cases, reduced number of hops or reduced number of retries, the typically slower but more reliable sub-GHz interface can positively affect the latency when considering the proposed dual-band operation.

V. Methodology

This section describes the methodology employed in the experiments conducted in this study. Next, the simulation environment, the 6TiSCH Simulator configuration, the simulation scenario, and the applied performance metrics are presented.

A. Simulation Environment

The 6TiSCH Simulator from [40] was used for obtaining experimental results. This simulator was created by researchers from the working group that developed 6TiSCH. Since it was used to create the standard, it is one of the most complete and accurate 6TiSCH simulators available, but it is focused on networking perspective. Due to this choice, some physical layer aspects are not evaluated in the simulator and consequently could not be assessed in our work: first, there is no energy consumption evaluation. Second, the slower 868MHz interface may increase interference between networks, but since 6TiSCH simulator can only simulate a network per run it only takes into account the number of nodes that transmitted in a given timeslot for detecting collisions. This approach is sufficient to guarantee reliable results when only one network is present in the region of interest, but should be expanded if the more general case of multiple networks is important in an specific situation. Even without energy analysis our paper can be useful to evaluate the performance of dual band TSCH networks in some applications like industrial actuators, light bulbs, smart meters, connected white goods and connected cars, where energy requirements for non-communication related system components already renders the use of small batteries unfeasible. These systems may benefit from reduced latency and improved reliability with a negligible increase of energy consumption when compared to the overall system consumption which, besides the communication system are composed, for example, of big electric motors, heating/cooling elements or high current LEDs.

For the physical layer, in addition to the default TSCH configuration for the 2.4GHz operating band and propagation model based on OpenMote [43] already available, a second sub-GHz configuration was added, based on the Texas Instruments CC1352R [44] radio operating in the 802.15.4g SUN PHY at 868MHz. Table I summarizes the configuration of the simulation environment.

B. 6TiSCH Configuration

Some changes were made to the default configuration of the 6TiSCH Simulator version 1.3.0 [45], as to allow the dual band operation proposed in this manuscript. Such changes are described below.

- The packet generation interval, T_a, was changed to 10 seconds in order to make the network traffic denser, and as a consequence, to increase collision and packet loss probability.

- The uniform variance, V, applied to the packet generation time, was set to zero to force equal packet generation times for both radio interfaces, as to guarantee that transmissions from the sub-GHz and the 2.4 GHz interfaces are concurrent.
- The maximum number of retransmissions (or retries), R_t, was configured as the recommended maximum number of link-layer retransmissions defined in RFC 8180 [26] (i.e., up to 3 retransmissions).
- The clock drift, C_d, between a device and its time reference neighbor, was set to zero to establish a controlled environment, so that packet losses are not due to synchronization errors.
- In order to account for the potential different network formation times in both operating bands, application packets were scheduled to wait a fixed time (as to make sure both networks are formed). Then, after such period, transmissions start simultaneously in both interfaces.

1) Propagation Model for 868 MHz: The 6TiSCH Simulator was designed by the 6TiSCH IETF working group with three major goals: compliance with the standard, scalability and simplicity. Path loss follows the Pister-Hack [39] model. To determine reception probability, RSSI values are first converted to PDR values based on a conversion table, which was obtained empirically in a real deployment utilizing the OpenMote devices. According to [46] the conversion table accurately reflects the relationship between RSSI and PDR in large indoor industrial scenarios at the 2.4GHz band. Therefore, to account for a different operating band a new conversion table is required, which is constructed by applying an offset to the original one based on the differences in radio sensitivity from each operating band devices. More specifically, it was applied a 13 dB offset regarding the difference from the default Texas Instruments CC2538 radio [47] sensitivity to that of the Texas Instruments CC1352R.

C. Simulation Scenario

With high reliability applications in mind, we simulated network topologies formed by three different network sizes $N \in \{40, 80, 160\}$. In conjunction with the chosen 10s message interval, these network sizes represent roughly 12.5%, 25%, 50% timeslot allocation at the DAG root, which guarantees that both networks (868MHz and 2.4GHz), in the worst load scenario, have enough spare resources to deliver downstream packets to every received upstream packet, which is important in wireless networked control applications, for example.

For each network size, two deployment models were deployed, namely Linear and Random. The simulation runs twice, first for 2.4 GHz band and then for 868 MHz band. Finally, metrics are combined to analyze the resulting network performance. Each simulation run spans for 7200s but the results from the first 5400s are considered a Warmup time and, for this reason, are not taken into account for the final results. We used this resource to let the network routes stabilize since we are most interested in the steady-state behavior of the network. We believe that an industrial network will usually run uninterruptedly for several days, and the network formation behavior should be disregarded. The scenario parameters are listed in Table I.

TABLE I: Simulation scenario parameters.

Parameters	Values
Network size	40-80-160 nodes
Area	100m $\times$ 100m
Warmup time (W)	5400s
Duration time	7200s
Message interval (T_a)	10s (uniform)
UDP payload	90 bytes
Retranssmissions (R)	3
Slotframe Size (J)	101 timeslots

VI. Simulation Results

This section presents the results of 36 simulated experiments, where the 12 different topologies were run 3 times with different random seeds [1]. The discussion regarding PDR and latency, for each individual interface and for the resulting multi-band network, is presented in the following subsections.

A. Packet Delivery Ratio

We initiate our discussions by first presenting results concerning the PDR for each combination of network size, operating band and deployment in Figs. 5 and 6. In addition to that, the associated joint metric resulted from the combination of both interfaces is also presented. It can be noticed that the PDR decreases with the network size, effect that is most significantly observed in the 2.4GHz band. The network size increase also degrades the joint metric results from multi-band support, yet the proposed configuration still considerably improves the overall performance. The most significant improvement is observed in the Linear deployment with 160 devices as demonstrated in Fig. 6. There, multi-band support improved PDR by 20% when compared to the single usage of 2.4GHz and close to 7% when compared to the single usage of 868MHz band. Similarly, multi-band support offered an increase of 4.84% and 7.09% in the PDR for the 40 and 80 network sizes using Linear deployments.

Regarding Random deployments, in most cases the same behavior was observed. The increase in network size resulted in lower network performance, while the multi-band support yielded significant improvements of 14.88% for the 160 node network, 10.05% and 6.99% for 80 and 40 node network, respectively.

Moreover, the reason for decreased performance over larger networks is that the more denser the network, the higher is the interference and the strain over bottlenecks nodes closer to the DAG root [49]. This loss in performance is most noticeable in 2.4GHz operating bands mainly due to its weaker sensitivity.

Tables II and III present the average, standard deviation, minimum and maximum values for the PDR, for the random and linear topologies, respectively, considering the three seeds, and for different number of nodes. As we can see, the multi band approach, besides being better in terms of average

[1]The source code used in this work is available at [48].

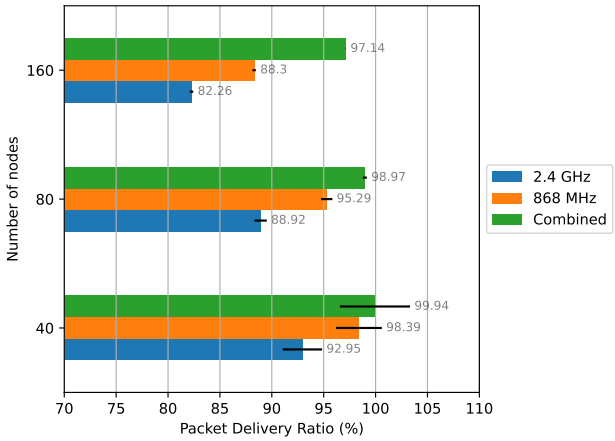

Fig. 5: PDR results for each operating band varying in network size with 40, 80 and 160 nodes deployed in a 100m × 100m area, in the random topology. Black lines are 95% confidence intervals.

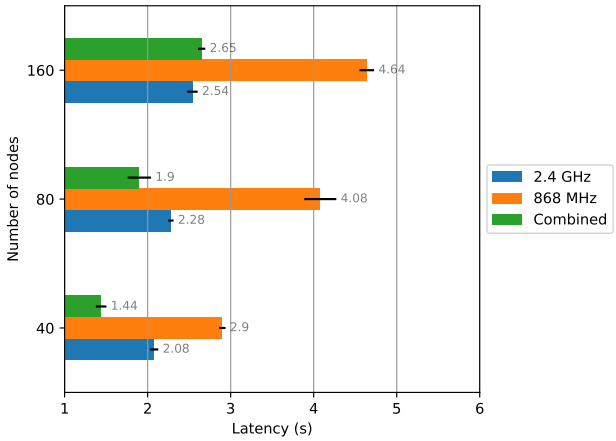

Fig. 7: Average latency results for each operating band varying in network size with 40, 80 and 160 nodes deployed in a 100m × 100m area, in the linear topology. Black lines are 95% confidence intervals.

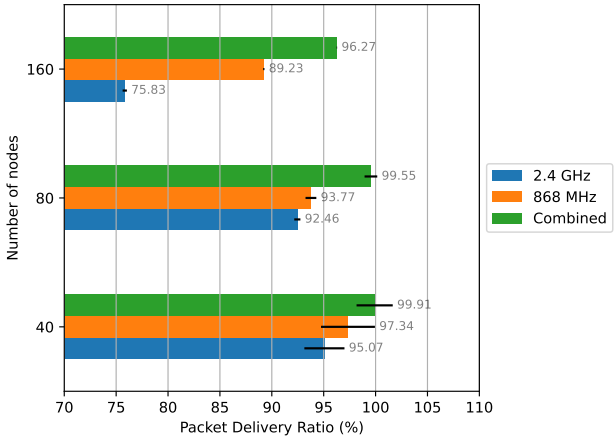

Fig. 6: PDR results for each operating band varying in network size with 40, 80 and 160 nodes deployed in a 100m × 100m area, in the linear topology. Black lines are 95% confidence intervals.

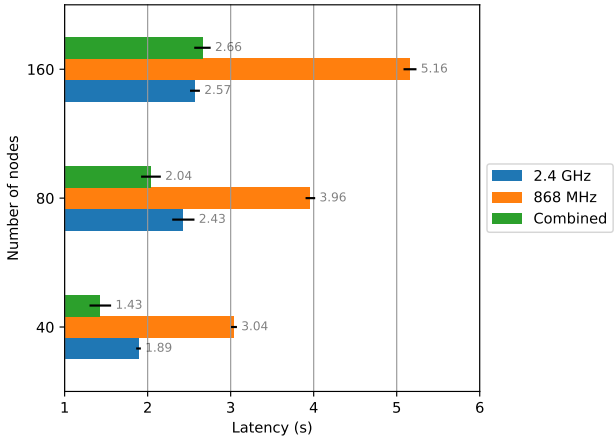

Fig. 8: Average latency results for each operating band varying in network size with 40, 80 and 160 nodes deployed in a 100m × 100m area, in the random topology. Black lines are 95% confidence intervals.

PDR, is also more homogeneous among different nodes and topology realizations, since the standard deviation is lower, while the minimum and maximum values are closer as well.

B. Latency

In terms of latency, similarly to the case of PDR, the increase in network size resulted in poorer overall network performance, while the multi-band support yielded significant improvements. Figs. 7 and 8 present the average latency for each operating band and the resulting joint metric in case of multi-band support. It can be noticed an improvement of 30.76% and 16.6% in the average latency by combining both operating bands when deploying Linear networks of size 40 and 80, respectively. Similar behavior was observed in the Random deployment, obtaining an improvement of 24.33% and 16.04% in the average latency with 40 and 80 nodes. This benefit is associated with reduced packet retransmissions and reduced average hop number in packet forwarding.

However, as shown in Fig. 7, one can observe a 4.33% degradation in the average latency for the joint metric when compared to the 2.4 GHz band in the 160 nodes scenario. This can be explained by the PDR reduction caused by the density increase of the network.

From Figs. 6 to 8 we can observe that, for the 868 MHz interface, the average latency and the PDR are always higher than those considering the 2.4 GHz interface. On the other hand, since both the combined latency and combined PDR could be reduced for the 40 and 80 nodes topologies, we can

	40 nodes			80 nodes			160 nodes		
Band	2.4 GHz	868 MHz	multi	2.4 GHz	868 MHz	multi	2.4 GHz	868 MHz	multi
avg	92.95%	98.39%	99.94%	88.92%	95.29%	98.97%	82.26%	88.30%	97.14%
s.d.	0.11059	0.00634	0.00059	0.07242	0.01771	0.00540	0.06193	0.01943	0.00566
min	80.20%	97.74%	99.88%	84.05%	93.28%	98.43%	75.24%	86.32%	96.50%
max	100.00%	99.01%	100.00%	97.24%	96.63%	99.51%	86.97%	90.21%	97.57%

TABLE II: PDR average (avg), standard deviation (s.d.), minimum (min) and maximum (max) values for random topologies with 40, 80 and 160 nodes, in a square area of 100 m $\times$ 100 m. The results consider three independent runs.

	40 nodes			80 nodes			160 nodes		
Band	2.4 GHz	868 MHz	multi	2.4 GHz	868 MHz	multi	2.4 GHz	868 MHz	multi
avg	95.07%	97.34%	99.91%	92.46%	93.77%	99.55%	75.83%	89.23%	96.27%
s.d.	0.05706	0.01998	0.00087	0.08494	0.01701	0.00200	0.06318	0.00968	0.00677
min	88.51%	95.20%	99.83%	82.68%	91.86%	99.32%	70.17%	88.54%	95.52%
max	98.81%	99.16%	100.00%	97.95%	95.14%	99.70%	82.65%	90.34%	96.82%

TABLE III: PDR average (avg), standard deviation (s.d.), minimum (min) and maximum (max) values for linear topologies with 40, 80 and 160 nodes, in a square area of 100 m $\times$ 100 m. The results consider three independent runs.

infer that eventually some packets are delivered faster by the 868 MHz interface than the 2.4 GHz interface. Although that may sound counterintuitive, it may be due to some packets that were transmitted in less hops in the 868 MHz interface than they would be in the 2.4 GHz interface, or because the 868 MHz required less retries due to its increased PDR. However, clearly, the 2.4 GHz interface contributes more to the good latency results than the 868 MHz interface. Nevertheless, in more demanding conditions, as in the case of the 160 nodes topology, the 2.4GHz network starts lowering its contribution to the overall metrics, and we observe a tendency of the numbers to drift towards the 868MHz typical performance. With a PDR of approximately 76% in the 160 nodes topology, the 2.4 GHz interface is not able to contribute to reduce the average latency, as almost 24% of the packets would be delivered exclusively by the 868 MHz interface, which is typically slower.

While the increase in average latency can appear to be harmful to the network, the increase in successfully received packets offered by combining both bands is essential to the correct execution of certain applications, thus representing an appealing trade-off.

Similar to the analysis of the PDR, Tables IV and V present the average, standard deviation, minimum and maximum values for the latency, for the random and linear topologies, respectively, considering the three seeds, and for different number of nodes. The conclusions are similar as, again, the multi band approach performs very well in terms of latency while being more homogeneous among different nodes and topology realizations.

C. Latency per Band

The experiments from Subsections VI-A and VI-B showed that multi-band support is beneficial for 6TiSCH networks and various industrial applications by providing frequency diversity and reducing interference from other technologies, thus increasing PDR. Also, multi-band support is useful in decreasing average packet retransmissions, allowing lower end-to-end latency in most cases. Next, the contributions of each band for the overall result are further investigated using a randomly deployed scenario with 40 nodes.

Table VI shows the total network packet retries and the average packet retransmissions by node for the proposed network, while Fig. 9 presents the latency Cumulative Distribution Function (CDF), both for each operating band and the resulting combined network. It can be seen from Table VI that the 868 MHz band required approximately only 47% of the number of retransmissions carried out by the 2.4 Ghz interface. Moreover, it is very interesting to note that the case of combined 868 MHz and 2.4 GHz interfaces required only 72% of the retransmissions carried out by the 2.4 GHz interface when utilized alone, what has positive implications in power consumption, for instance. Furthermore, the similarity between combined and 2.4GHz Latency CDF curves from 0 to 1s in Fig. 9 indicates that the faster transmission times and shorter slotframe duration are the major players providing the lowest latency paths towards the DAG root. However, as illustrated in Fig. 10, it is interesting to note that 11 out of the 39 nodes had a lower average latency in the 868 Mhz band, representing 28% of the nodes. This shows that the sub-GHz band also helps in reducing the average network latency.

D. Node Density

In the experiments from Subsections VI-A and VI-B the simulation area was kept fixed in 100m x 100m while increasing the number of nodes, which means that the distances between the nodes changes and the density changes as well. Since the 2.4GHz band has lower range, its reliability in the denser configurations may be improved since distances are smaller. To investigate the impact of this effect, we have also performed tests where we change the simulation area as to maintain the node density per square meter constant when the number of nodes increases.

Somewhat surprising, for every simulated number of nodes, the PDR of the less dense experiment was better than that in the denser network with closer nodes, as can be seen in Figs. 6 and 11. Such behavior may be explained because, due to scheduling and the retry mechanism, the main source of

KPIs	40 nodes			80 nodes			160 nodes		
Band	2.4 GHz	868 MHz	multi	2.4 GHz	868 MHz	multi	2.4 GHz	868 MHz	multi
avg	1.89s	3.04s	1.43s	2.43s	3.96s	2.04s	2.57s	5.16s	2.66s
s.d.	0.42303	0.38817	0.32503	0.11544	0.18689	0.24592	0.09485	0.43543	0.19283
min	1.47s	2.61s	1.06s	2.35s	3.64s	1.75s	2.49s	4.66s	2.46s
max	2.32s	3.37s	1.63s	2.56s	3.99s	2.24s	2.67s	5.46s	2.85s

TABLE IV: Latency average (avg), standard deviation (s.d.), minimum (min) and maximum (max) values for random topologies with 40, 80 and 160 nodes, in a square area of 100 m $\times$ 100 m. The results consider three independent runs.

KPIs	40 nodes			80 nodes			160 nodes		
Band	2.4 GHz	868 MHz	multi	2.4 GHz	868 MHz	multi	2.4 GHz	868 MHz	multi
avg	2.08s	2.90s	1.44s	2.28s	4.08s	1.90s	2.54s	4.64s	2.65s
s.d.	0.21099	0.45650	0.14827	0.12291	0.63091	0.28894	0.15739	0.10442	0.20355
min	1.85s	2.44s	1.30s	2.18s	3.35s	1.59s	2.40s	4.54s	2.46s
max	2.26s	3.36s	1.59s	2.42s	4.51s	2.16s	2.71s	4.75s	2.87s

TABLE V: Latency average (avg), standard deviation (s.d.), minimum (min) and maximum (max) values for linear topologies with 40, 80 and 160 nodes, in a square area of 100 m $\times$ 100 m. The results consider three independent runs.

TABLE VI: Packet retries for the scenario with 40 nodes in a random topology.

Metric	2.4 Ghz	868 Mhz	Combined
Network total	506	237	364
Average by node	12.97	6.07	9.333

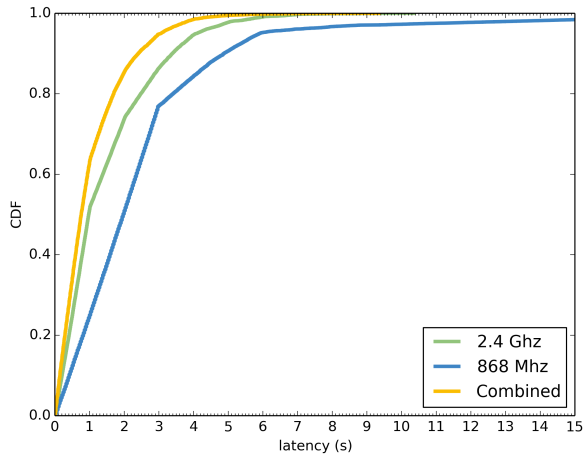

Fig. 9: Latencies CDF for the scenario with 40 nodes in a random topology.

packet losses on a 6TiSCH network is queue congestion. On a less dense network, the traffic is more evenly spread because every node has less forwarding options, which reduces the packet losses due to congestion. On the other hand, since the nodes are farther away, more retransmissions occur, leading to a higher latency, which can be This work was partially funded by Brazilian National Council for Scientific and Technological Development - CNPq, grant 402378/2021-0.observed in Figs. 7 and 12. Nevertheless, the general conclusions about the improvements of our technique on the combined metrics are the same as in the experiments with fixed area and increased node density.

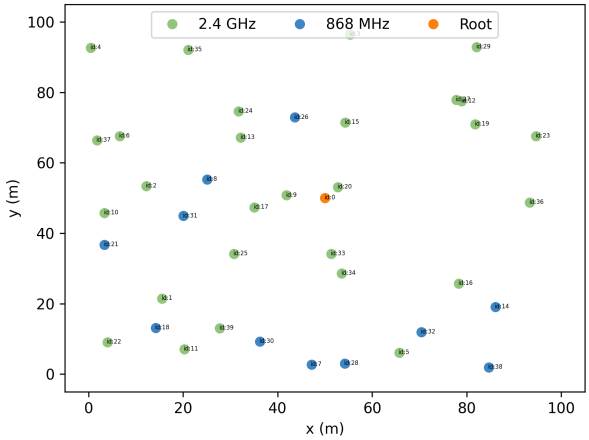

Fig. 10: Random deployment of 40 devices in a 100m $\times$ 100m area, highlighting the operating band that delivered the lowest average latency on each device.

VII. Conclusions

This work proposed the addition of a second radio interface in network devices to operate a redundant 6TiSCH network in sub-GHz bands. Results show an increase of 20% in PDR and closely to 31% decrease in latency in some scenarios. The gains are associated with diversity from a redundant transmission and physical link characteristics present in the sub-GHz band, which lead to an increased reliability and longer range. All in all, the two operating bands offer distinct trade-offs regarding reliability and latency, while the combination of both can improve overall network performance for 6TiSCH networks. The following is a summary of the advantages and drawbacks of the proposed scheme:

- Advantages: a) increases PDR by adding diversity and utilizing sub-Ghz bands that offer greater robustness against propagation losses; b) reduces latency by selecting the first received packet from either operating band; c) reduces the amount of retransmissions, decreasing

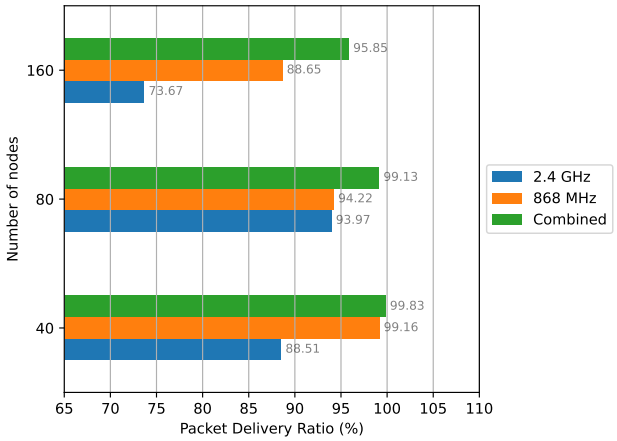

Fig. 11: PDR for the 868 MHz and the 2.4 GHz interfaces, as well as for the multi band operation, for the 40, 80 and 160 nodes linear topologies considering constant node density, so that the area increases with the number of nodes.

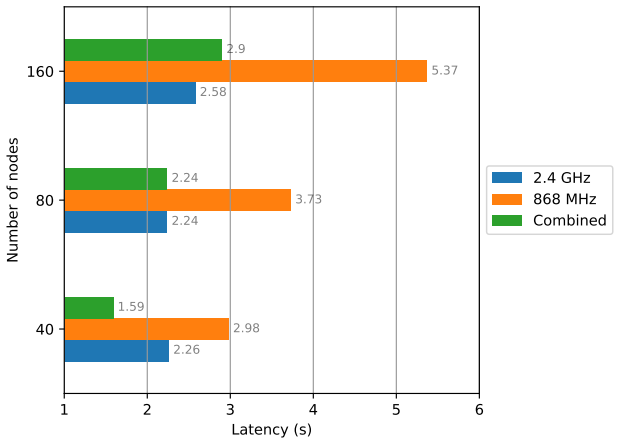

Fig. 12: Latency for the 868 MHz and the 2.4 GHz interfaces, as well as for the multi band operation, for the 40, 80 and 160 nodes linear topologies, considering constant node density, so that the area increases with the number of nodes.

congestion, latency and consumption.

- Drawbacks: a) requires a second radio interface at the nodes; b) increases the energy consumption as all packets are transmitted in a redundant form; c) increases application complexity in the border router or application server to manage and discard duplicated packets.

In future works the proposed method could be tested in large-scale topologies with hardware heterogeneity and in real environments. Moreover, dynamic radio selection could be investigated in combination with IPv6 packet tagging allowing diverse application QoS levels. Finally, additional studies are required to better comprehend the effects of TSCH and RPL networks regarding packet queue lengths and transmissions retries to prevent network bottlenecks.

REFERENCES

[1] G. L. Moritz, M. Bunn, R. D. Souza, and S. Mafra, "Improving 6TiSCH Reliability and Latency with Simultaneous Multi-Band Operation," in *Anais do XL Simpósio Brasileiro de Telecomunicações e Processamento de Sinais*. Sociedade Brasileira de Telecomunicações, 2022. doi: 10.14209/sbrt.2022.1570814882. [Online]. Available: https://biblioteca.sbrt.org.br/articles/3585

[2] R. Drath and A. Horch, "Industrie 4.0: Hit or hype? [industry forum]," *IEEE Ind. Electron. Mag.*, vol. 8, no. 2, pp. 56–58, 2014. doi: 10.1109/mie.2014.2312079

[3] M. Hermann, T. Pentek, and B. Otto, "Design principles for industrie 4.0 scenarios," in *2016 49th Hawaii international conference on system sciences (HICSS)*. IEEE, 2016. doi: 10.1109/hicss.2016.488 pp. 3928–3937.

[4] S. Vitturi, F. Tramarin, and L. Seno, "Industrial wireless networks: The significance of timeliness in communication systems," *IEEE Ind. Electron. Mag.*, vol. 7, no. 2, pp. 40–51, 2013. doi: 10.1109/mie.2013.2253837

[5] V. C. Gungor and G. P. Hancke, "Industrial wireless sensor networks: Challenges, design principles, and technical approaches," *IEEE Trans. Ind. Electron.*, vol. 56, no. 10, pp. 4258–4265, 2009. doi: 10.1109/tie.2009.2015754

[6] R. Candell and M. Kashef, "Industrial wireless: Problem space, success considerations, technologies, and future direction," in *2017 Resilience Week (RWS)*. IEEE, 2017. doi: 10.1109/rweek.2017.8088661 pp. 133–139.

[7] D. Chen, M. Nixon, and A. W. Mok, "Real-time mesh network for industrial automation," 2010, springer: Berlin/Heidelberg, Germany.

[8] ISA100 Wireless Compliance Institute, "Wireless systems for industrial automation: Process control and related applications," https://isa100wci.org/, 2009, accessed on: November 5, 2021.

[9] "Wireless communication network and communication profiles - WIA-PA," International Electrotechnical Commission, Geneva, CH, International Standard, 2015.

[10] "IEEE standard for low-rate wireless networks," pp. 1–709, 2016.

[11] T. Watteyne, J. Weiss, L. Doherty, and J. Simon, "Industrial IEEE802.15.4 e networks: Performance and trade-offs," in *2015 IEEE International Conference on Communications (ICC)*. IEEE, 2015. doi: 10.1109/icc.2015.7248388 pp. 604–609.

[12] R. Yu, "Mesh network protocols for the industrial internet of things," *Microwave Journal*, vol. 57, no. 12, pp. 38–+, 2014.

[13] IEEE Standards Association, "IEEE is fueling the fourth industrial revolution," https://innovate.IEEE.org/innovation-spotlight-IEEE-fueling-fourth-industrial-revolution/, 2020, accessed on: November 5, 2021.

[14] X. Vilajosana, T. Watteyne, M. Vučinić, T. Chang, and K. S. Pister, "6TiSCH: Industrial performance for ipv6 internet-of-things networks," *Proc. IEEE*, vol. 107, no. 6, pp. 1153–1165, 2019. doi: 10.1109/jproc.2019.2906404

[15] D. Dujovne, T. Watteyne, X. Vilajosana, and P. Thubert, "6TiSCH: deterministic ip-enabled industrial internet (of things)," *IEEE Commun. Mag.*, vol. 52, no. 12, pp. 36–41, 2014. doi: 10.1109/mcom.2014.6979984

[16] C. Lu, A. Saifullah, B. Li, M. Sha, H. Gonzalez, D. Gunatilaka, C. Wu, L. Nie, and Y. Chen, "Real-time wireless sensor-actuator networks for industrial cyber-PHYsical systems," *Proc. IEEE*, vol. 104, no. 5, pp. 1013–1024, 2016. doi: 10.1109/JPROC.2015.2497161

[17] P. Minet, I. Khoufi, and A. Laouiti, "Increasing reliability of a TSCH network for the industry 4.0," in *2017 IEEE 16th International Symposium on Network Computing and Applications (NCA)*, 2017. doi: 10.1109/NCA.2017.8171344 pp. 1–10.

[18] G. Z. Papadopoulos, T. Matsui, P. Thubert, G. Texier, T. Watteyne, and N. Montavont, "Leapfrog collaboration: Toward determinism and predictability in industrial-iot applications," in *2017 IEEE International Conference on Communications (ICC)*, 2017. doi: 10.1109/ICC.2017.7997160 pp. 1–6.

[19] S. Yin, O. Gnawali, P. Sommer, and B. Kusy, "Multi channel performance of dual band low power wireless network," in *2014 IEEE 11th International Conference on Mobile Ad Hoc and Sensor Systems*, 2014. doi: 10.1109/MASS.2014.120 pp. 345–353.

[20] M. Brachmann, S. Duquennoy, N. Tsiftes, and T. Voigt, "IEEE 802.15.4 TSCH in sub-GHz: Design considerations and multi-band support," in *2019 IEEE 44th Conference on Local Computer Networks (LCN)*, 2019. doi: 10.1109/LCN44214.2019.8990806 pp. 42–50.

[21] L. Pelusi, A. Passarella, and M. Conti, "Opportunistic networking: data forwarding in disconnected mobile ad hoc networks,"

IEEE Commun. Mag., vol. 44, no. 11, pp. 134–141, 2006. doi: 10.1109/MCOM.2006.248176

[22] I. Akyildiz and X. Wang, "A survey on wireless mesh networks," *IEEE Commun. Mag.*, vol. 43, no. 9, pp. S23–S30, 2005. doi: 10.1109/MCOM.2005.1509968

[23] M. Vucinic, J. Simon, K. Pister, and M. Richardson, "Constrained join protocol (cojp) for 6TiSCH," Working Draft, IETF Secretariat, Internet-Draft draft-ietf-6TiSCH-minimal-security-15, December 2019, http://www.ietf.org/internet-drafts/draft-ietf-{6TiSCH}-minimal-security-15.txt. [Online]. Available: http://www.ietf.org/internet-drafts/draft-ietf-{6TiSCH}-minimal-security-15.txt

[24] T. Chang, M. Vucinic, X. Vilajosana, S. Duquennoy, and D. Dujovne, "6TiSCH minimal scheduling function (msf)," Working Draft, IETF Secretariat, Internet-Draft draft-ietf-6TiSCH-msf-18, September 2020, http://www.ietf.org/internet-drafts/draft-ietf-{6TiSCH}-msf-18.txt. [Online]. Available: http://www.ietf.org/internet-drafts/draft-ietf-{6TiSCH}-msf-18.txt

[25] T. Kivinen and P. Kinney, "IEEE 802.15.4 information element for the IETF," Internet Requests for Comments, RFC Editor, RFC 8137, May 2017.

[26] K. Pister and T. Watteyne, "Minimal IPv6 over the TSCH mode of IEEE 802.15.4e (6TiSCH) configuration," Internet Requests for Comments, RFC Editor, BCP 210, May 2017.

[27] X. Vilajosana and T. Watteyne, "6TiSCH operation sublayer (6top) protocol (6p)," Internet Requests for Comments, RFC Editor, RFC 8480, November 2018.

[28] X. Vilajosana, T. Watteyne, T. Chang, M. Vučinić, S. Duquennoy, and P. Thubert, "Ietf 6TiSCH: A tutorial," *IEEE Commun. Surv. Tutorials*, vol. 22, no. 1, pp. 595–615, 2020. doi: 10.1109/COMST.2019.2939407

[29] A. Brandt, J. Hui, R. Kelsey, P. Levis, K. Pister, R. Struik, and R. A. and, "RPL: IPv6 routing protocol for low-power and lossy networks," Internet Requests for Comments, RFC Editor, RFC 6550, March 2012, http://www.rfc-editor.org/rfc/rfc6550.txt. [Online]. Available: http://www.rfc-editor.org/rfc/rfc6550.txt

[30] H. Pereira, G. L. Moritz, R. D. Souza, A. Munaretto, and M. Fonseca, "Increased network lifetime and load balancing based on network interface average power metric for RPL," *IEEE Access*, vol. 8, pp. 48 686–48 696, 2020. doi: 10.1109/access.2020.2979834

[31] N. Kushalnagar, G. Montenegro, and C. Schumacher, "IPv6 over low-power wireless personal area networks (6lowpans): Overview, assumptions, problem statement, and goals," Internet Requests for Comments, RFC Editor, RFC 4919, August 2007, http://www.rfc-editor.org/rfc/rfc4919.txt. [Online]. Available: http://www.rfc-editor.org/rfc/rfc4919.txt

[32] Z. Shelby, K. Hartke, and C. Bormann, "The constrained application protocol (CoAP)," Internet Requests for Comments, RFC Editor, RFC 7252, June 2014, http://www.rfc-editor.org/rfc/rfc7252.txt. [Online]. Available: http://www.rfc-editor.org/rfc/rfc7252.txt

[33] G. Selander, J. Mattsson, F. Palombini, and L. Seitz, "Object security for constrained RESTful environments (OSCORE)," Internet Requests for Comments, RFC Editor, RFC 8613, July 2019.

[34] Q. Li, D. Han, O. Gnawali, P. Sommer, and B. Kusy, "Twonet: Large-scale wireless sensor network testbed with dual-radio nodes," in *Proceedings of the 11th ACM Conference on Embedded Networked Sensor Systems*, 2013. doi: 10.1145/2517351.2517440 pp. 1–2.

[35] R. Jurdak, K. Klues, B. Kusy, C. Richter, K. Langendoen, and M. Brunig, "Opal: A multiradio platform for high throughput wireless sensor networks," *IEEE Embedded Sys. Lett.*, vol. 3, no. 4, pp. 121–124, 2011. doi: 10.1109/LES.2011.2177065

[36] D. Van Leemput, J. Bauwens, R. Elsas, J. Hoebeke, W. Joseph, and E. De Poorter, "Adaptive multi-PHY IEEE802.15.4 TSCH in sub-GHz industrial wireless networks," *Ad Hoc Networks*, vol. 111, p. 102330, 2021. doi: https://doi.org/10.1016/j.adhoc.2020.102330. [Online]. Available: https://www.sciencedirect.com/science/article/pii/S157087052030682X

[37] M. Rady, Q. Lampin, D. Barthel, and T. Watteyne, "g6TiSCH: Generalized 6TiSCH for agile multi-PHY wireless networking," *IEEE Access*, vol. 9, pp. 84 465–84 479, 2021. doi: 10.1109/ACCESS.2021.3085967

[38] ——, "Bringing life out of diversity: Boosting network lifetime using multi-PHY routing in RPL," *Transactions on Emerging Telecommunications Technologies*, vol. 33, no. 11, p. e4592, 2022. doi: https://doi.org/10.1002/ett.4592. [Online]. Available: https://onlinelibrary.wiley.com/doi/abs/10.1002/ett.4592

[39] H.-P. Le, M. John, and K. Pister, "Energy-aware routing in wireless sensor networks with adaptive energy-slope control," *EE290Q-2 Spring*, 2009.

[40] E. Municio, G. Daneels, M. Vučinić, S. Latré, J. Famaey, Y. Tanaka, K. Brun, K. Muraoka, X. Vilajosana, and T. Watteyne, "Simulating 6TiSCH networks," *Transactions on Emerging Telecommunications Technologies*, vol. 30, no. 3, p. e3494, 2019. doi: 10.1002/ett.3494

[41] Microchip Corporation, "AT86RF215, Sub-1GHz/2.4GHz Transceiver and I/Q Radio for IEEE Std 802.15.4-2015, IEEE Std 802.15.4g-2012, ETSI TS 102 887-1," https://www.microchip.com/content/dam/mchp/documents/OTH/ProductDocuments/DataSheets/Atmel-42415-WIRELESS-AT86RF215_Datasheet.pdf, accessed on: November 5, 2021.

[42] "IEEE standard for local and metropolitan area networks–part 15.4: Low-rate wireless personal area networks (lr-wpans) amendment 3: PHYsical layer (PHY) specifications for low-data-rate, wireless, smart metering utility networks," *IEEE Std 802.15.4g-2012 (Amendment to IEEE Std 802.15.4-2011)*, pp. 1–252, 2012. doi: 10.1109/ieeeSTD.2012.6190698

[43] X. Vilajosana, P. Tuset, T. Watteyne, and K. Pister, "Openmote: Open-source prototyping platform for the industrial iot," in *International Conference on Ad Hoc Networks*. Springer, 2015. doi: 10.1007/978-3-319-25067-0_17 pp. 211–222.

[44] T. Instruments, "CC1352R simplelink™ high-performance multi-band wireless mcu," https://www.ti.com/lit/ds/symlink/CC1352R.pdf, 2018, accessed on: November 5, 2021.

[45] Y. Tanaka, K. Brun, M. Vučinić, and T. Watteyne, "The 6TiSCH simulator," https://bitbucket.org/{6TiSCH}/simulator/src/v1.3.0/, accessed on: November 5, 2021.

[46] K. Brun-Laguna, A. L. Diedrichs, D. Dujovne, R. Leone, X. Vilajosana, and T. Watteyne, "(not so) intuitive results from a smart agriculture low-power wireless mesh deployment," in *Proceedings of the Eleventh ACM Workshop on Challenged Networks*, 2016. doi: 10.1145/2979683.2979696 pp. 25–30.

[47] Texas Instruments, "CC2538 powerful wireless microcontroller system-on-chip for 2.4-GHz IEEE 802.15.4," https://www.ti.com/lit/ds/symlink/cc2538.pdf, accessed on: November 5, 2021.

[48] Marcus Bunn, "Multi-band support for the 6TiSCH simulator," https://github.com/bunnmv/6TiSCH-simulator/tree/sub-GHz, accessed on: November 5, 2021.

[49] H. Farag, P. Österberg, and M. Gidlund, "Congestion detection and control for 6TiSCH networks in iiot applications," in *ICC 2020 - 2020 IEEE International Conference on Communications (ICC)*, 2020. doi: 10.1109/ICC40277.2020.9149365 pp. 1–6.

Marcus V. Bunn was born in São José, Brazil, in 1993. He received the B.Sc. in Telecommunications Engineering from the Federal Institute of Santa Catarina (IFSC), São José, Brazil, in 2018 and a M.Sc. degree in Electrical Engineering from the Federal University of Santa Catarina (UFSC) in 2021. His research interests are in the area of wireless communications and the Internet of Things.

Richard Demo Souza (IEEE S'01–M'04–SM'12) received the D.Sc. degree in Electrical Engineering from the Federal University of Santa Catarina (UFSC), Brazil, in 2003. From 2004 to 2016 he was with the Federal University of Technology – Paraná (UTFPR), Brazil. Since 2017 he has been with UFSC, where he is a Professor in the Department of Electrical and Electronics Engineering. His research interests are in the areas of wireless communications and signal processing. He has served as Editor or Associate Editor for the SBrT Journal of Communications and Information Systems, the IEEE Communications Letters, the IEEE Transactions on Vehicular Technology, the IEEE Transactions on Communications, and the IEEE Internet of Things Journal. He is the supervisor of the awarded Best PhD Thesis in Electrical Engineering in Brazil in 2014, and a co-recipient of the 2016 Research Award from the Cuban Academy of Sciences.

Guilherme Luiz Moritz was born in Gaspar, Brazil, in 1984. He received the B.Sc. and the D.Sc. degrees in electrical engineering from the Federal University of Technology-Paraná (UTFPR), Curitiba, Brazil, in 2012 and 2015, respectively, where he is currently an Assistant Professor of embedded systems, control systems, and wireless sensor networks. His research interests are in the area of wireless communications, cooperative communications, and the Internet of Things.

Samuel Baraldi Mafra received the B.Sc. degree from the Santa Catarina State University (UDESC), Joinville, Brazil in 2010, the M.Sc. degree from the Federal University of Parana (UFPR), Curitiba, Brazil in 2012, and the D.Sc. degree from the Federal University of Technology—Parana (UTFPR), Curitiba, Brazil, in 2015, all in electrical engineering. He held a Post-Doctoral position at the UFPR in the period from September 2015 to May 2018. He is currently an Assistant Professor at the Inatel -National Institute of Telecommunications. His research interests lie in the broad area of wireless communication theory, with applications to cognitive radio networks and cooperative communications. He is a member of the IEEE Communications Society and Brazilian Telecommunications Society (SBrT).